Towards Computationally Efficient Dynamic Model of a Planar Parallel Continuum Robot

Mohamed Rekkal, Gowrishankar Ganesh, and João Cavalcanti Santos

Abstract This article explores a computationally efficient dynamic model for a planar parallel continuum robot composed of two slender elastic links. Each link is modeled using a planar Kirchhoff formulation, enabling bending deformations along one axis while neglecting other deformations. Static equilibrium is computed through direct spatial integration of the rod equations combined with optimization-based single-shooting, in which unknown boundary forces and moments are adjusted to satisfy end-effector compatibility and equilibrium conditions. A suitable dynamic model is introduced by concentrating inertia and damping at the end-effector, while assuming quasi-static link deformation. As the resulting model do not have inertia distributed along elastic elements, the differential equations related to deformation and dynamic effects are decoupled. Therefore, the original problem that would lead to partial differential equations, is approximated by two sets of ordinary differential equations. Accordingly, time integration and quasi-static rod equilibrium are recomputed alternately at each time step. To overcome the limitations of penalty-based single-shooting, a multiple shooting formulation is further proposed, enforcing continuity and equilibrium along the link length through intermediate nodes. The proposed method represents an intermediary step towards a computationally efficient dynamic model of parallel continuum robots.

M. Rekkal
University of Montpellier, UM-CNRS LIRMM, France
e-mail: mohamed.rekkal@lirmm.fr

G. Ganesh
CNRS, UM-CNRS LIRMM, France
e-mail: ganesh.gowrishankar@lirmm.fr

J. Cavalcanti Santos
University of Montpellier, UM-CNRS LIRMM, France
e-mail: joao.cavalcanti-santos@lirmm.fr

1 Introduction

Parallel Continuum Robots (PCRs) are complex robotic mechanisms introduced with the expectation to operate in the blind spots of rigid-link robot functionality. Their mobility arises from flexible slender elements assembled into closed kinematic chains. As a result, PCRs combine the structural benefits of parallel architectures with the compliance of continuum and compliant mechanisms. By virtue of their architecture, PCRs may offer advantageous characteristics. In particular, compliant robots are well suited for confined environments due to their nonlinear deformation capabilities and ease of miniaturization. Parallel continuum architectures further enhance stiffness while preserving passive compliance, enabling higher manipulation forces with many degrees of freedom. These valuable assets place PCRs as noteworthy candidates in areas such as surgery [?] and teleoperated flexible platforms [?]. Depending on their design, PCRs may exhibit improved positioning precision compared to conventional continuum robots [?].

The study of PCRs represents a promising yet maturing field, facing persistent modeling and control challenges. Early works proposed constant-curvature models [?], which describe the structure of each beam as a succession of smooth arc-shaped segments. Similarly, the continuous deformation of a beam can be discretized as several rigid links connected by passive elastic joints, so that a PCR is modeled as an hyper-redundant mechanism [?]. More advanced formulations consider geometrically exact Cosserat rod dynamics, incorporating distributed actuation and energy-based force models [?]. Recasting Cosserat-rod statics as optimal-control or variational problems is also common [?], enabling stability assessment via second-order sufficiency conditions.

Nevertheless, achieving a balance between physical fidelity, numerical robustness, and computational efficiency remains an open problem, particularly for parallel continuum architectures undergoing significant accelerations. The dynamics of a PCR couples distributed deformation and inertia. Therefore, an exact model should include derivatives with respect to both space and time, capturing elasticity and dynamic effects, respectively. Typically, the resulting partial differential equations (PDEs) are able to represent the dynamics of a single beam. The complete model of a PCR should incorporate such PDEs while enforcing equality constraints that impose the geometric relation between the multiple kinematic chains. Indeed, recent studies show that even elaborate and efficient methods struggle to model relatively simple systems in real time [?]. This makes the model-based control of PCRs undergoing high accelerations prohibitive.

This work presents intermediate results aiming at a compromise between precision and computational efficiency. A dynamic model of the planar PCR studied in [?] and [?] is established by decoupling elasticity and dynamic effects. The mass of the beams is assumed to be significantly lower than the inertia of the end-effector, which is a reasonable hypothesis when dealing with sufficiently slender rods and relatively heavy loads. Concentrating the dynamic effects in the end-effector, the elastic elements are modeled using a static model. This model computes the efforts applied by the rods to the end-effector, which is then used to determine its motion using simple Newtonian dynamics. In summary, two different systems of *ordinary* differential equations are dealt with alternately.

The remainder of this article is organized as follows. Section 2 formulates an optimization problem able to solve the statics of the studied PCR considering Kirchhoff beam model and a single-shooting method. The resulting static model is then used in Section 3 to integrate the end-effector motion over time. Since single-shooting methods may suffer from numerical robustness issues, Section 4 proposes an alternative formulation applying multiple shooting. Finally, conclusions and perspectives are presented in Section 5.

2 Statics

The planar two-rod parallel continuum robot illustrated in Figure 1 is considered. The same mechanism was studied in [**?**] and [**?**], and Campa *et al.* applied a similar architecture for pick-and-place tasks in [**?**].

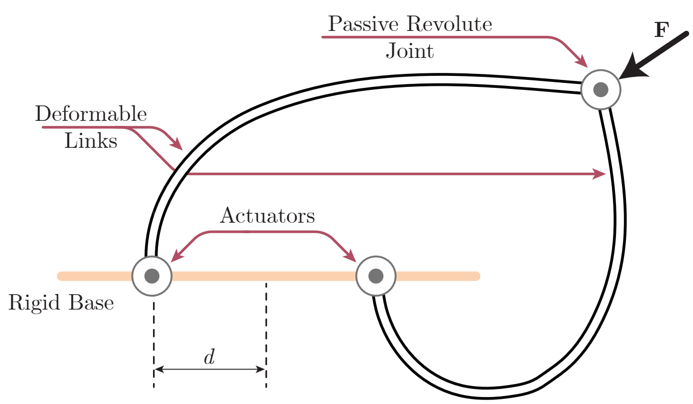

Fig. 1 An illustration of the studied planar two-rod parallel continuum robot.

Each link is modeled as a planar Kirchhoff rod parameterized by arc length $s \in [0, L]$, with centerline $\mathbf{r}(s) = [x(s) \quad y(s)]^\top$ and orientation $\theta(s)$ satisfying

$$\frac{dx}{ds} = \cos\theta(s), \qquad \frac{dy}{ds} = \sin\theta(s). \tag{1}$$

The curvature is

$$\kappa(s) = \frac{d\theta}{ds} = \frac{m(s)}{EI}, \tag{2}$$

where m is the bending moment and EI the bending stiffness. Assuming that no external *distributed* effort is applied, moment and force equilibria yield

$$\frac{dm}{ds} = n_x \sin\theta(s) - n_y \cos\theta(s). \tag{3}$$

where n_x and n_y denote the constant internal forces along the Cartesian axes. The system of ordinary differential equations composed of (1)-(3) can be numerically integrated for known initial conditions at $s = 0$.

The robot consists of two identical links $i \in \{1, 2\}$ of length L, attached to the base at $\mathbf{r}_1(0) = [-d \quad 0]^\top$ and $\mathbf{r}_2(0) = [d \quad 0]^\top$, respectively, with d the distance defined in Figure 1. The state vector of beam i is defined as $\mathbf{y}_i(s) = [x_i \quad y_i \quad \theta_i \quad m_i]^\top$, which collects the variables to be integrated using (1)-(3) over $s \in [0, L]$. More precisely, the state $\mathbf{y}_i(s)$ of each beam i should satisfy

$$\frac{d\mathbf{y}_i}{ds} = \mathbf{f}\big(\mathbf{y}_i(s)\big) = [\cos\theta_i \quad \sin\theta_i \quad m_i/EI \quad n_{x,i}\sin\theta_i - n_{y,i}\cos\theta_i]^\top \tag{4}$$

with $\mathbf{f} : \mathbb{R}^4 \to \mathbb{R}^4$ defined according to (1)-(3).

The present section addresses the problem of finding the rod configurations $\mathbf{y}_1(s),\ \mathbf{y}_2(s)$ for a known end-effector position $\mathbf{r}_1(L) = \mathbf{r}_2(L) = \mathbf{r}_d = [x_d \ \ y_d]^\top$ and motor positions $\theta_i(0) = q_i$. To do so, one may collect all independent unknown variables in $\mathbf{Y} = [n_{x,1} \quad n_{y,1} \quad n_{x,2} \quad n_{y,2} \quad m_{0,1} \quad m_{0,2} \quad F_x \quad F_y]$, with $m_{0,i} = m_i(0)$ and $\mathbf{F} = [F_x \quad F_y]^\top$ the force applied on the passive revolute joint, as illustrated in Figure 1. The vector $\mathbf{Y}$ satisfying the proposed constraints can be obtained by solving the optimization problem given by

$$\min_{\mathbf{Y}} \ w_{\text{pos}} J_{\text{pos}} + w_{\text{mom}} J_{\text{mom}} + w_{\text{force}} J_{\text{force}} \tag{5a}$$

$$\text{s.t. } \frac{d\mathbf{y}_i(s)}{ds} = \mathbf{f}\big(\mathbf{y}_i(s)\big) \tag{5b}$$

$$\theta_i(0) = q_i \tag{5c}$$

with cost terms defined as

$$J_{\text{pos}} = \sum_{i=1}^{2} \left[(x_d - x_i(L))^2 + (y_d - y_i(L))^2\right], \tag{6a}$$

$$J_{\text{mom}} = m_1(L)^2 + m_2(L)^2, \tag{6b}$$

$$J_{\text{force}} = (n_{x,1} + n_{x,2} + F_x)^2 + (n_{y,1} + n_{y,2} + F_y)^2 \tag{6c}$$

in which (6) define the objective terms: (6a) penalizes tip position error, (6b) enforces the zero distal-moment condition induced by the passive revolute joint and (6c) promotes force balance between external forces applied at the tip of the rods $\mathbf{F} = [F_x \quad F_y]^\top$ and internal forces $n_{x,i}$, $n_{y,i}$. The weights w_{pos}, w_{mom}, w_{force} are tuned to improve numerical convergence. Figure 2 exemplifies a numerical example obtained with the proposed approach.

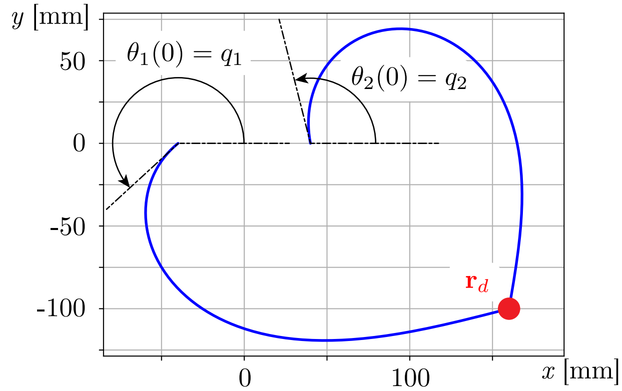

Fig. 2 Quasi-static equilibrium of a planar PCR with strictly positive w_{pos}, w_{mom} and w_{force} using single-shooting

3 Dynamics

The rods are assumed to have negligible inertia relative to the end effector. Therefore, rod mass is neglected and the end-effector inertia is treated as dominant. Under this assumption, the rod configurations can be deduced taking into account statics only, and the solution of (5) is valid for known end-effector position $\mathbf{r}_d$ and motor positions q_i.

In particular, the solution of (5) determines the force $\mathbf{F}$ exerted on the passive revolute joint. Representing the end-effector as a lumped mass attached to the passive revolute joint, its equations of motion can be derived via simple Newtonian mechanics. Thus, end-effector position $\mathbf{p}(t)$ should satisfy

$$m\,\ddot{\mathbf{p}} + c\,\dot{\mathbf{p}} = -\mathbf{F} + \mathbf{F}_{ext} \tag{7}$$

where m denotes the lumped end-effector mass, c is a viscous damping coefficient representing non-conservative phenomena and $\mathbf{F}_{ext}$ an external force. The resulting equations are integrated using semi-implicit Euler method, with the quasi-static link equilibrium (5) recomputed at each time step. Figure 3 illustrates the resulting trajectory of the tip response for an initial velocity different from the equilibrium position.

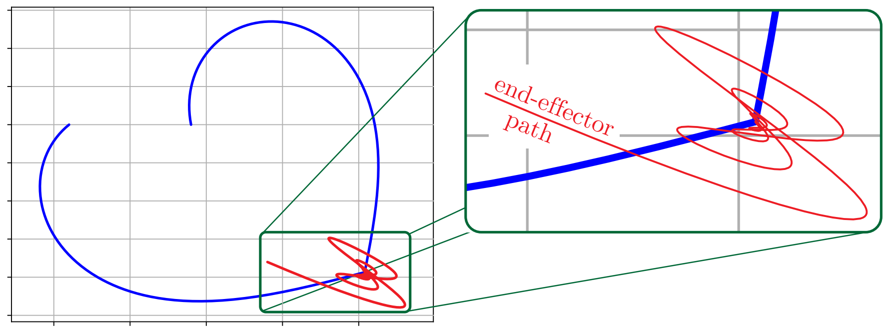

Fig. 3 End-effector response obtained with the proposed decoupled dynamic model.

4 Multiple Shooting Formulation

To improve numerical robustness under poor initial guesses, a multiple-shooting method (MSM) is introduced to compute quasi-static equilibria of the planar two-rod mechanism. MSM advances the solution via sequential propagation along a discretized arc length. The links are partitioned into segments, and the system state is propagated from base to tip while enforcing continuity of internal variables through residual constraints at intermediate nodes. End-effector compatibility and global equilibrium are imposed simultaneously, ensuring geometric and physical consistency across the segments.

Each link $i \in \{1, 2\}$ is discretized along the arc length $s \in [0, L]$ into N segments of equal length $L_{\mathrm{seg}} = L/N$, with nodes $s_k = kL_{\mathrm{seg}}$. At each node, the internal variables

$$\mathbf{u}_{i,k} = \left[\theta_{i,k},\, n_{x,i,k},\, n_{y,i,k},\, m_{i,k}\right]^{\top}, \qquad k = 0, \ldots, N-1, \tag{8}$$

are treated as decision variables. The centerline position is not optimized directly; instead, it is obtained by forward integration of the Kirchhoff rod equations.

The base position and orientation of each link are prescribed, defining $\mathbf{r}_i(0)$ and $\theta_i(0)$. Let $\mathbf{y}_{i,k} = [\mathbf{r}_{i,k}^{\top} \;\; \mathbf{u}_{i,k}^{\top}]^{\top}$ denote the full rod state at node k. The nodal positions $\mathbf{r}_{i,k}$ are not decision variables and are obtained recursively by propagation, with $\mathbf{r}_{i,0} = \mathbf{r}_i(0)$.

The global decision vector is

$$\mathbf{Y} = \begin{bmatrix} \mathbf{u}_{1,0}^\top & \dots & \mathbf{u}_{1,N-1}^\top & \mathbf{u}_{2,0}^\top & \dots & \mathbf{u}_{2,N-1}^\top \end{bmatrix}^\top \in \mathbb{R}^{8N}. \tag{9}$$

Given the state at s_k, the rod equations are integrated over one segment to obtain

$$\mathbf{y}_{i,k}^{\text{end}} = \begin{bmatrix} \mathbf{r}_{i,k}^{\text{end}} \\ \mathbf{u}_{i,k}^{\text{end}} \end{bmatrix} = \Phi(\mathbf{y}_{i,k}; L_{\text{seg}}), \tag{10}$$

where $\Phi(\mathbf{y}_0; L_{\text{seg}})$ denotes the solution of the Kirchhoff rod initial value problem evaluated at arclength L_{seg} with initial condition $\mathbf{y}(0) = \mathbf{y}_0$.

Continuity of the internal variables is enforced through the residual

$$\mathbf{e}_{i,k}^{\text{cont}} = \mathbf{u}_{i,k+1} - \mathbf{u}_{i,k}^{\text{end}}, \qquad k = 0, \dots, N-2. \tag{11}$$

Geometric continuity follows by construction since $\mathbf{r}_{i,k}^{\text{end}}$ initializes the next segment. Let $\mathbf{r}_i(L)$, $\mathbf{n}_i(L)$, and $m_i(L)$ denote the tip position, force, and moment of link i, with $\mathbf{n}_i(L) = [n_{x,i}(L) \;\; n_{y,i}(L)]^\top$. The corresponding residuals are

$$\mathbf{e}^{\text{pos}} = \begin{bmatrix} \mathbf{r}_1(L) - \mathbf{r}_d \\ \mathbf{r}_2(L) - \mathbf{r}_d \end{bmatrix}, \tag{12}$$

$$\mathbf{e}^{\text{force}} = \mathbf{n}_1(L) + \mathbf{n}_2(L) + \mathbf{F}, \tag{13}$$

$$\mathbf{e}^{\text{mom}} = \begin{bmatrix} m_1(L) \\ m_2(L) \end{bmatrix}. \tag{14}$$

All residuals are assembled into

$$\mathbf{R}(\mathbf{Y}) = \left[\{\mathbf{e}_{i,k}^{\text{cont}}\}, \sqrt{w_{\text{pos}}}\mathbf{e}^{\text{pos}}, \sqrt{w_{\text{force}}}\mathbf{e}^{\text{force}}, \sqrt{w_{\text{mom}}}\mathbf{e}^{\text{mom}}\right]^{\mathsf{T}}, \tag{15}$$

where $w_{\text{pos}}, w_{\text{force}}, w_{\text{mom}}$ weight geometric and equilibrium constraints.

The equilibrium configuration is obtained from

$$\mathbf{Y}^\star = \arg\min_{\mathbf{Y}} \frac{1}{2}\|\mathbf{R}(\mathbf{Y})\|_2^2. \tag{16}$$

The nonlinear least-squares problem is solved iteratively by forward integrating the rod equations over all segments, evaluating continuity and boundary residuals, and updating $\mathbf{Y}$ until convergence. This yields a quasi-static equilibrium satisfying rod mechanics, segment continuity, and closed-chain constraints. Figure 4 shows a rendered solution for an imposed end-effector position $(0.18, 0.12)$.

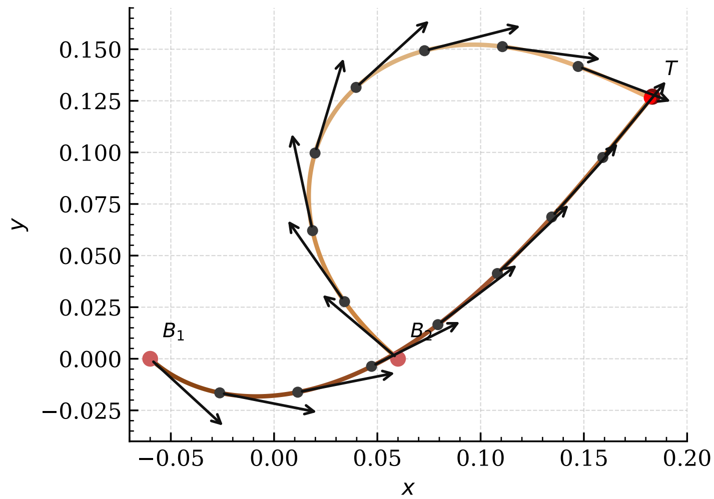

Fig. 4 Multiple shooting method solution for a planar PCR (using $N = 8$ nodes)

5 Conclusion

This article presents an exploratory, lightweight dynamic model of a planar PCR governed by the Kirchhoff rod equations. The approximate model neglects link mass, assuming that the system inertia is dominated by the end-effector. Consequently, link shapes are reconstructed quasi-statically. A multiple shooting formulation is introduced to improve numerical robustness under large deformations and poor initial guesses. Future work will focus on assessing the accuracy and computational efficiency of the proposed method through comparisons with baseline simulation frameworks and experimental validation. The proposed approximate model is indented to be integrated into model-based control strategies requiring significantly low computational cost, such as MPC.

References

1. Altuzarra, O., Caballero, D., Campa, F.J., Pinto, C.: Position analysis in planar continuum mechanisms. Mechanism and Machine Theory **136**, 68–82 (2019)
2. Anderson, P.L., Mahoney, A.W., Webster, R.J.: Continuum reconfigurable parallel robots for surgery: Shape sensing and state estimation with uncertainty. IEEE Robotics and Automation Letters **2**(3), 1427–1434 (2017)
3. Boyer, F., Gotelli, A., Tempel, P., Lebastard, V., Renda, F., Briot, S.: Implicit Time-Integration Simulation of Robots With Rigid Bodies and Cosserat Rods Based on a Newton–Euler Recursive Algorithm **40**, 677–696 (2024). DOI 10.1109/TRO.2023.3334647

4. Briot, S., Boyer, F.: A geometrically exact assumed strain modes approach for the geometrico-and kinemato-static modelings of continuum parallel robots. IEEE Transactions on Robotics **39**(2), 1527–1543 (2022)
5. Campa, F.J., Diez, M., Diaz-Caneja, D., Altuzarra, O.: A 2 Dof Continuum Parallel Robot for Pick & Place Collaborative Tasks. In: T. Uhl (ed.) Advances in Mechanism and Machine Science, vol. 73, pp. 1979–1988. Springer International Publishing (2019). DOI 10.1007/978-3-030-20131-9_196
6. Chen, G., Zhang, Z., Chen, Z., Wang, H.: A General Discretization-Based Approach for the Kinetostatic Analysis of Closed-Loop Rigid/Flexible Hybrid Mechanisms. In: J. Lenarcic, V. Parenti-Castelli (eds.) Advances in Robot Kinematics 2018, pp. 269–276. Springer International Publishing. DOI 10.1007/978-3-319-93188-3_31
7. Lilge, S., Nuelle, K., Childs, J.A., Wen, K., Rucker, D.C., Burgner-Kahrs, J.: Parallel-continuum robots: A survey. IEEE Transactions on Robotics **40**, 3252–3270 (2024)
8. Till, J., Rucker, D.C.: Elastic stability of cosserat rods and parallel continuum robots. IEEE Transactions on Robotics **33**(3), 718–733 (2017)
9. Till, J.D.: On the statics, dynamics, and stability of continuum robots: Model formulations and efficient computational schemes. Ph.D. thesis, University of Tennessee, Knoxville, TN, USA (2019)
10. Webster, R.J., Jones, B.A.: Design and kinematic modeling of constant curvature continuum robots: A review. International Journal of Robotics Research **29**(13), 1661–1683 (2010)
11. Zaccaria, F., Idà, E., Briot, S.: Directional Critical Load Index: A Distance-to-Instability Metric for Continuum Robots **40**, 3620–3637 (2024). DOI 10.1109/TRO.2024.3428432